

Measurement of liver iron overload by magnetic induction using a planar gradiometer: preliminary human results

R Casañas^{1,3}, H Scharfetter², A Altes⁴, A Remacha⁴, P Sarda⁴, J Sierra⁴,
R Merwa², K Hollaus⁵ and J Rosell³

¹ Escuela de Bioanálisis, Facultad de Medicina, Universidad Central de Venezuela, Caracas, Venezuela

² Institute for Biomedical Engineering, Graz University of Technology, 8010 Graz, Austria

³ Departament d'Enginyeria Electrònica, Universitat Politècnica de Catalunya, 08034 Barcelona, Spain

⁴ Departamento de Hematología, Hospital de la Santa Creu i Sant Pau, Barcelona, Spain

⁵ Institute for Fundamentals and Theory in Electrical Engineering, IGTE, Graz University of Technology, 8010 Graz, Austria

Received 31 July 2003, accepted for publication 12 September 2003

Published 3 February 2004

Online at stacks.iop.org/PM/25/315 (DOI: 10.1088/0967-3334/25/1/035)

Abstract

The measurement of hepatic iron overload is of particular interest in cases of hereditary hemochromatosis or in patients subject to periodic blood transfusion. The measurement of plasma ferritin provides an indirect estimate but the usefulness of this method is limited by many common clinical conditions (inflammation, infection, etc). Liver biopsy provides the most quantitative direct measurement of iron content in the liver but the risk of the procedure limits its acceptability. This work studies the feasibility of a magnetic induction (MI) low-cost system to measure liver iron overload. The excitation magnetic field (B_0 , frequency: 28 kHz) was produced by a coil, the perturbation produced by the object (ΔB) was detected using a planar gradiometer. We measured ten patients and seven volunteers in supine and prone positions. Each subject was moved in a plane parallel to the gradiometer several times to estimate measurement repeatability. The real and imaginary parts of $\Delta B/B_0$ were measured. Plastic tanks filled with water, saline and ferric solutions were measured for calibration purposes. We used a finite element model to evaluate the experimental results. To estimate the iron content we used the ratio between the maximum values for real and imaginary parts of $\Delta B/B_0$ and the area formed by the Nyquist plot divided by the maximum imaginary part. Measurements in humans showed that the contribution of the permittivity is stronger than the contribution of the permeability produced by iron stores in the liver. Defined iron estimators show a limited correlation with expected iron content in patients ($R \leq 0.56$). A more precise control of geometry and position of the subjects and measurements at multiple frequencies would improve the method.

Keywords: magnetic induction, susceptibility measurements, hemochromatosis, hepatic iron

(Some figures in this article are in colour only in the electronic version)

1. Introduction

The measurement of hepatic iron overload is of particular interest in cases of hereditary hemochromatosis, thalassemia major, aplastic anemia or in patients subject to periodic blood transfusion. Measurement of body iron is essential for managing iron-chelating therapy in these patients. The measurement of plasma ferritin provides an indirect estimate but the usefulness of this method is limited by many common clinical conditions (inflammation, infection, etc). Liver biopsy provides the most quantitative direct measurement of iron content in the liver but the risk of the procedure limits its acceptability. In a recent meeting (Brittenham and Badman 2003) it was concluded that there is a clear clinical need for a quantitative, non-invasive and safe method to estimate body storage iron to improve the diagnostic and management of these patients.

The first non-invasive *in vivo* induction methods, for iron overload measurement, were tried in animals by Bauman and Hoffman (1967). The same group published a study of the magnetic parameters of hepatic iron stores in humans (Bauman and Harris 1967), which established the value of iron concentration and magnetic susceptibility for normal human hepatic tissue.

Non-invasive measurement techniques studied up to now are MRI and magnetic susceptometry. Magnetic susceptometry systems are based on SQUIDs and are the only non-invasive method that has been validated and used in clinical studies (Paulson *et al* 1991, Brittenham *et al* 1982). Major problems of this technique are the need for a cryogenic region to place the SQUIDs and the use of a special screened room to avoid electromagnetic interference. The problems of magnetic resonance imaging (Gandon *et al* 1994) are cost, difficulties in making quantitative measurements and poor reproducibility (Brittenham and Badman 2003).

In vitro standard methods for *in vitro* measurement are histological studies with hematoxylin–eosin and Perls' Prussian blue and biochemical measurements (Brissot *et al* 1981).

The possibility of applying magnetic induction (MI) methods for the measurement of the electrical conductivity in poorly conducting samples ($\sigma \leq 2 \text{ S m}^{-1}$) was demonstrated theoretically (Griffiths *et al* 1999) and experimentally (Scharfetter *et al* 2001a). The potential of MI techniques to characterize paramagnetic and diamagnetic materials *in vitro* has been proved theoretically and experimentally by Casañas *et al* (2001).

In this work, we describe the basic principles, the measurement protocols and the experimental prototype developed for this application. Results for *in vivo* MI measurements on models and humans are given.

2. Materials and methods

2.1. Mathematical model

Consider two coils positioned coaxially (figure 1) and spaced by a distance $2a$. A sinusoidal current, of angular frequency ω , in the excitation coil produces a magnetic field B_0 that is measured at the receiver coil. Both coils are supposed to have a small radius with respect

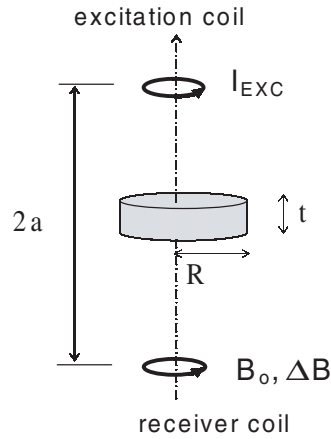


Figure 1. Coil-coil system.

to their distance and are modelled as magnetic dipoles. Suppose a circular disc of radius R , thickness t ($t \ll 2a$), conductivity σ , permittivity $\epsilon_0\epsilon_r$ and relative permeability μ_r , is placed coaxially and centrally between the coils. The magnetic field B_0 will induce eddy currents and magnetization in the disc. Eddy currents produce a perturbation ΔB_e of B_0 (Griffiths *et al* 1999). Moreover, a magnetic field is created in the plane of the disc that magnetizes it, causing an additional perturbation ΔB_m in the sensing coil. The total relative perturbation ($(\Delta B_e + \Delta B_m)/B_0$) due to eddy currents and the magnetization, in the sensing coil (z component only), is (Casañas *et al* 2001, Scharfetter *et al* 2003)

$$\frac{\Delta B_t}{B_0} = \frac{\Delta V}{V_0} = \frac{a^3 t}{2} \left\{ \chi \frac{R^2(8a^2 - R^2)}{(a^2 + R^2)^4} - j(\sigma + j2\pi f \epsilon_0 \epsilon_r) 2\pi f \mu_0 \frac{R^4}{a^2(a^2 + R^2)^2} \right\} \quad (1)$$

where χ is the magnetic susceptibility of the material ($\chi = \mu_r - 1$) and f the magnetic field frequency.

If the object is not centred and a gradiometer is used the constants determined by the geometric factors (a, R, t) will change and the general expression will be

$$\frac{\Delta B_t}{B_0} = k_2 \chi + 2\pi k_1 \epsilon_0 \epsilon_r f^2 - j k_1 \sigma f \quad (2)$$

where k_1 and k_2 are constants related to the geometry of the coils and the object respectively. This equation is valid for homogeneous objects in the empty space.

The perturbation produced by a paramagnetic ($\chi > 0$) or diamagnetic ($\chi < 0$) conductor is reflected in the real part of the total perturbation $\text{Re}(\Delta B_t/B_0)$ together with the contribution of the electrical permittivity $\epsilon_0\epsilon_r$. $\text{Im}(\Delta B_t/B_0)$ will essentially contain information about the conductivity σ .

2.2. Finite element model

To evaluate the expected signals for *in vivo* measurements we used the finite element method. The programme for solving the electromagnetic quasi-static eddy-current problem was developed at the Graz University of Technology. We modelled the thorax and abdomen as a cylinder ($R = 12$ cm, $L = 60$ cm) and the liver as a non-centred sphere ($R = 6.5$ cm) inside it (figure 2). The surrounding space (free space) is a sphere of 2 m in diameter. The sensor was modelled as a planar gradiometer (Rosell *et al* 2001). We simulated different positions

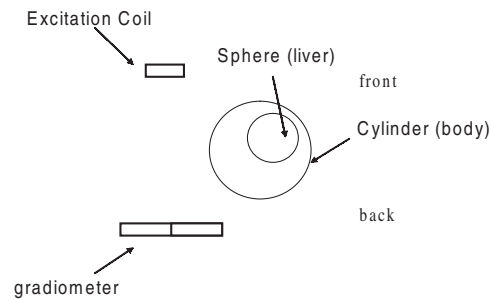


Figure 2. Finite element method: model geometry. Thorax and abdomen were modelled as a cylinder and the liver as a non-centred sphere.

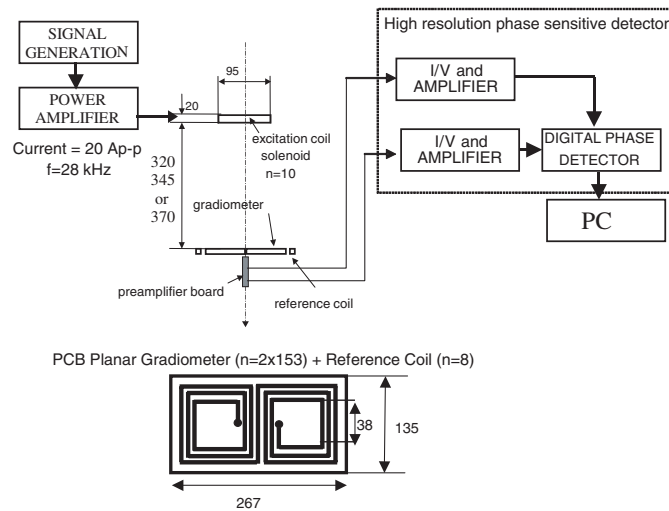


Figure 3. Measurement system using a coil as excitation and a planar gradiometer as receiver. All measures in millimetres.

(prone, supine and lateral displacements of the body in relation to the excitation and detection coils) and as a function of the electrical properties (σ , ϵ_r , μ_r) of both materials: the liver and the body.

2.3. Instrumentation system

The experimental system (electronic circuits and algorithms) described in Scharfetter (2001b) was used after adapting the data acquisition system and the excitation circuit to achieve maximum sensitivity and allow the measurement of the subjects (figure 3). The distance between excitation coil and gradiometer was increased to a minimum of 32.0 cm, but two more separations (34.5 and 37.0 cm) were used in the case of subjects with higher thorax perimeters. To compensate the linear decrease of the induced voltage with the frequency we designed a new gradiometer with 153 turns (each side) and a reference coil with 8 turns. We incorporated a board for digital coherent demodulation (Bocanegra and Riu 1995) allowing an acquisition speed of 100 measurements per second. We use two pre-amplifiers with differential current outputs, one for the signal coming from the gradiometer and the other for the reference. The pre-amplifier board was located in the zone of low sensitivity (figure 3) of the gradiometer

Table 1. Patients.

Alias	Sex	Weight (kg)	Height (cm)	Extracted Fe (g)	Fe concentration ($\mu\text{mol Fe/g}$)
Ll1	F	64	158	4.8	
Me1	M	75	168	1.3	
Ti1	F	50	150	6.0	66.7
Ar1	M	85	172	3.8	
Fu1	M	85	170	4.0	
Pa1	M	80	170	6.5	
Re1	M	84	176	1.0	15.1
Se1	M	80	175	3.0	
Pa2	M	80	170	4.7	
Pa3	M	80	170	0.0	
De1	M	88	173	6.0	

Table 2. Volunteers.

Alias	Sex	Weight (kg)	Height (cm)
Mi1	M	78	163
Sa1	F	57	165
Al2	M	87	175
An1	M	80	178
He1	M	51	167
Ro1	M	84	177
Xa1	M	72	169

very close to it. The differential current output, in conjunction with a shielded twisted pair cable, provides high immunity against electromagnetic interference.

2.4. Subjects

We measured ten patients with a positive diagnosis of hemochromatosis (table 1) and seven volunteers (table 2) presumed normal. After the MI measurement, all patients were subject to periodic phlebotomy until the ferritin level was lower than $50 \mu\text{g}$ of Fe. In table 1 the total extracted iron during the whole treatment is given. One of the patients (Pa) was measured three times during the phlebotomy treatment. One of the patients was excluded for further analysis because he had a hip prosthesis which perturbed the MI measurements dramatically. Only in two cases did we have a liver biopsy before the MI measurements.

2.5. Measurement protocol

The subject was lying, in a supine or prone position, upon a movable wood table. He or she was positioned to locate the liver (localized by palpation) in the maximum sensitivity region of the gradiometers. They were requested to breathe normally and not to move during the manoeuvre. Then the table was moved in a plane parallel to the gradiometer. The displacement began at a position far away from the gradiometer (zero sensitivity). Then the subject entered the negative sensitivity region and after arriving at the positive sensitivity region was moved back to the initial position. The displacement was done manually trying to maintain a constant speed.

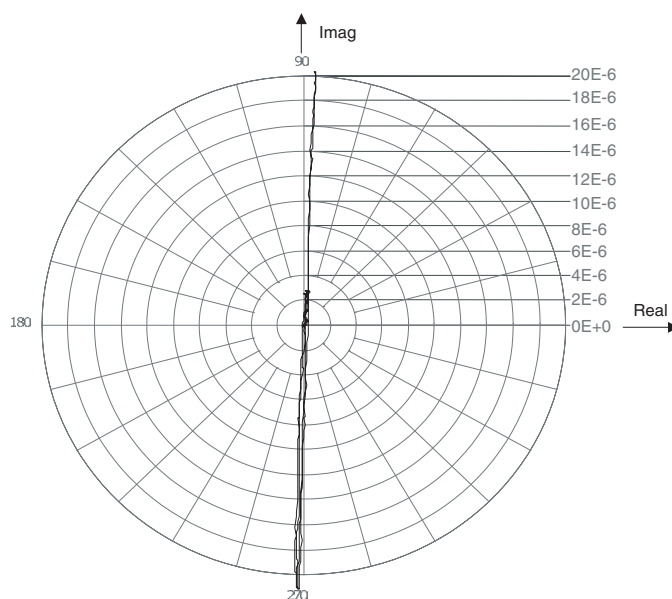


Figure 4. Nyquist diagram for a 50 l water tank with a conductivity of 0.4 S m^{-1} . Water is diamagnetic with a susceptibility of 10×10^{-6} . The graphic shows the trajectory of the real (x -axis) and imaginary parts (y -axis) of the detected signal in the gradiometer when the tank is moved as described in the protocol.

During this displacement real and imaginary components were detected and stored at a rate of 100 measurements per second.

To evaluate the response of the systems we also measured tanks with distilled water and solutions of FeCl_3 and NaCl at different concentrations.

3. Results

We measured a 50 l plastic tank filled with a solution of NaCl . The measured conductivity was 0.4 S m^{-1} (CRISON model GLP32, Spain). The expected magnetic susceptibility for this solution is 10×10^{-6} . Results are shown in a Nyquist diagram in figure 4. The graphic shows the trajectory of the real (x -axis) and imaginary parts (y -axis), of the detected signal in the gradiometer, when the object is moved as described in the protocol.

All subjects were measured at least three consecutive times in both positions: supine and prone. We found a clear difference between supine and prone positions. This difference could be seen in the Nyquist diagram in figure 5 for one of the normal subjects. In the supine position the loop appearing in the fourth quadrant was always bigger than in the prone position.

Using the FE model described we calculated the expected signals for different combinations of conductivity, permittivity and permeability. The combinations of these parameters that give a closer magnetic response to the experimental data in humans are shown in table 3.

Liver (D) represents a normal liver with normal iron content. An iron concentration of less than $15 \mu\text{mol Fe/g}$ dry liver is considered normal. The magnetic susceptibility for this iron concentration is negative (diamagnetic) with a value around -8.4×10^{-6} (Bauman and Harris 1967, Bauman and Hoffman 1967), which is close to the value 10×10^{-6} in the model. Liver (P) represents a paramagnetic liver with a strong iron overload ($540 \mu\text{mol Fe/g}$ dry liver).

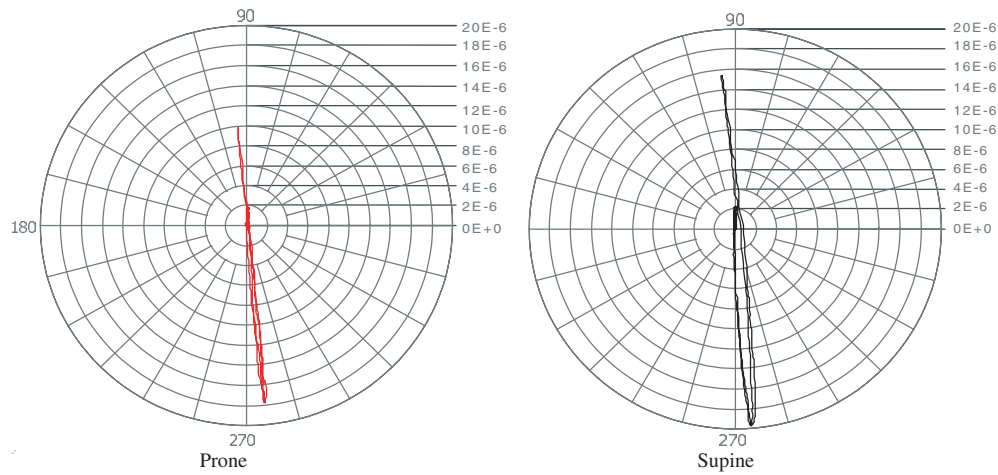


Figure 5. Nyquist diagram for one of the volunteers in the supine and prone positions when moved as the water tank in figure 4.

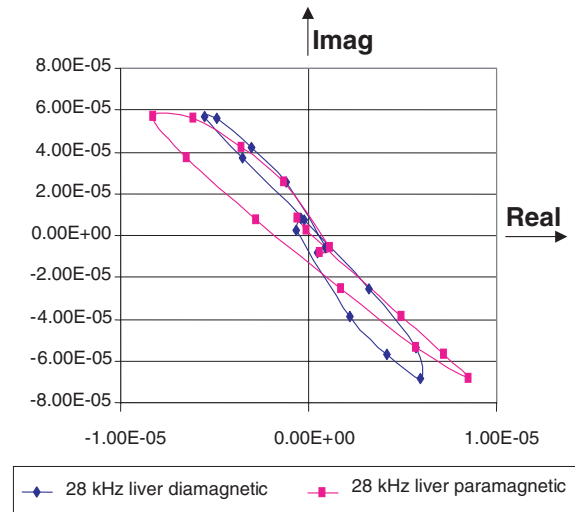


Figure 6. Nyquist diagram of the detected signal using the FEM when the object is moved as described in the protocol. The real part and also the shape of the loop changes depending on the iron content in the liver. Note that the real and imaginary scales are not equal.

Table 3. Conductivity, relative permittivity and susceptibility used in the FE model.

	σ (S m ⁻¹)	ϵ_r	χ
Body	0.1	10 000	-10×10^{-6}
Liver (P)	0.6	20 000	10×10^{-6}
Liver (D)	0.6	20 000	-10×10^{-6}

The results for these two simulations are plotted in a Nyquist diagram (figure 6) for the prone position (with the liver closer to the gradiometer).

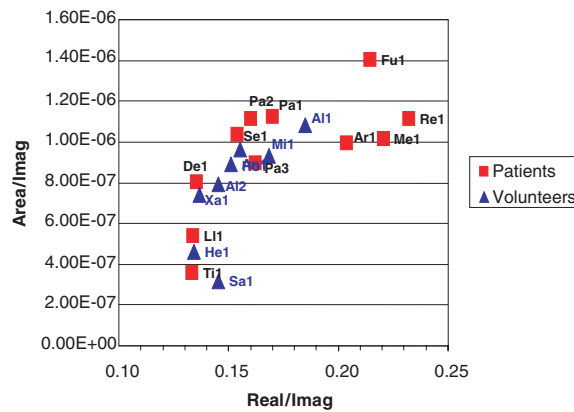


Figure 7. Separation between volunteers and patients using the defined estimators.

We also simulated the 50 l tank filled with saline of 0.4 S m^{-1} , relative permittivity of 80 and a susceptibility of 10×10^{-6} . In this case the results in the Nyquist diagram describe a straight line as expected and in agreement with the experimental measurement (figure 4).

From observation of the curves two preliminary estimators were defined and evaluated. The first is the maximum real part divided by the maximum imaginary part (R/I). The second is the area of the ellipse in the fourth quadrant divided by the maximum imaginary part (A/I). In both cases, all the measurements for each subject in the supine and prone positions were averaged. The separation between groups using these estimators is shown in figure 7. Considering only the patients the correlation coefficient between the extracted Fe and the estimator R/I was 0.53 (prone) and 0.47 (supine) respectively. Averaging the prone and supine positions was 0.56. The correlation coefficient for the A/I was 0.53 in the prone position and 0.03 in the supine position.

4. Discussion and conclusion

Measurements in different conditions: empty space, water tanks of different sizes, magnetic and diamagnetic materials, etc, were carried out to assure the proper operation of the system and to discard non-magnetic effects such as capacitive coupling.

The experimental and FE results obtained for a 50 l saline tank (figure 5) are in agreement with the mathematical model given in equations (1) and (2). When the sensitivity of the system is positive (k_1 and k_2 positive) the imaginary part must be negative (σ is always positive) and the real part must be negative if the susceptibility is negative (diamagnetic object).

For measurements in humans, we obtain a positive real part of $\Delta B_t/B_0$ while the imaginary part is negative. The latter is in agreement with the existence of conductive eddy currents in the body (Scharfetter *et al* 2003). Taking into account equations (1) and (2) a positive real part is only possible if the object is either paramagnetic (susceptibility >0) or the contribution of the dielectric eddy currents due to the high permittivity is higher than the negative susceptibility contribution due to diamagnetism.

The simulations using the FE model show that relative permittivities in the body must be in the order of 10 000 to 20 000 to explain the experimental results for humans. These values at 28 kHz are in agreement with previous studies and support the hypothesis that at this frequency (28 kHz), the human body is diamagnetic and the contribution of the permittivity term is dominant.

As the dependence on the frequency is different for each of the three electrical parameters (conductivity, permittivity and susceptibility), it seems feasible to separate their contributions using measurements at multiple frequencies. However, the strong changes of permittivity in biological tissues at low frequencies will make this separation more difficult.

Using the proposed estimators, only four patients are clearly separated from the volunteers. It seems that the weight of the subject has some effect on the estimators. For example, the three subjects with lower weight are in the lower corner in figure 7. This shows that other estimators taking into account the geometry of the subject (thorax diameter, weight, exact positions of the body, etc) must be developed to improve the accuracy of the method.

In conclusion, to evaluate new estimators and their uncertainty the *in vivo* study must be extended using: lower or multiple frequencies, more precise control of the geometry and position of the subject and subjects with known iron content.

Acknowledgments

This work was supported by the Austrian Science Foundation FWF, project P14990, by the Spanish CICYT, project SAF2001-1660, the Pathological Anatomic Service of the Sant Pau Hospital, Barcelona, Spain and the Advice of Scientific and Humanistic Development (CDCH), Central University of Venezuela. The authors thank Alfonso Mendez (UPC) for his excellent technical support.

References

- Bauman J H and Harris J W 1967 Estimation of hepatic iron stores by *in vivo* measurement of magnetic susceptibility *J. Lab. Clin. Med.* **70** 246–57
- Bauman J H and Hoffman R W 1967 Magnetic susceptibility meter for *in vivo* estimation of iron stores *IEEE Trans. Biomed. Eng.* **14** 239–43
- Bocanegra J M and Riu P 1995 Demodulador coherente basado en procesador digital de señales en la banda de 1 kHz a 1 MHz *Proyecto de Fin de Carrera Escola Tècnica Superior d'Enginyers de Telecomunicació, Universitat Politècnica de Catalunya*
- Brissot P, Bournel M, Henry D, Verger J P, Messner M, Beaumont C, Regnourard F, Ferrand B and Simon M 1981 Assessment of liver iron content in 271 patients: and evaluation of direct and indirect methods *Gastroenterology* **80** 557–65
- Brittenham G M and Badman D G 2003 Noninvasive measurement of iron: report of an NIDDK workshop *Blood* **101** 15–9
- Brittenham G M, Farrell D E, Harris J W, Feldman E S, Danish E H, Muir W A, Tripp J H and Bellon E M 1982 Magnetic-susceptibility measurement of human iron stores *New England J. Med.* **307** 1671–5
- Casañas R, Scharfetter H, Altes A and Rosell J 2001 Magnetic induction system for the non-invasive measurement of susceptibility and conductivity of biological tissues *Proc. 11th Conf. on Electrical Bio-Impedance* pp 623–6
- Gandon Y, Guyader D, Heautot J F, Reda M I, Yaouang J, Buhe T, Brissot P, Carsin M and Dugnier Y 1994 Hemochromatosis: diagnosis and quantification of liver iron with gradient–echo MR imaging *Radiology* **193** 533–8
- Griffiths H, Stewart W R and Gough W 1999 Magnetic induction tomography. A measuring system for biological tissue *Ann. NY Acad. Sci.* **873** 335–45
- Paulson D N, Fagaly R L, Toussaint R M and Fischer R 1991 Biomagnetic susceptometer with SQUID instrumentation *IEEE Trans. Magn.* **27** 3249–52
- Rosell J, Casañas R and Scharfetter H 2001 Sensitivity maps and systems requirements in magnetic induction tomography using a planar gradiometer *Physiol. Meas.* **22** 121–30
- Scharfetter H, Casañas R and Rosell J 2001b Systematic measurement errors in multi-frequency magnetic induction tomography (MIT) *Proc. 11th Conf. on Electrical Bio-Impedance* pp 415–9
- Scharfetter H, Casañas R and Rosell J 2003 Biological tissue characterization by magnetic induction spectroscopy (MIS): requirements and limitations *IEEE Trans. Biomed. Eng.* **50** 870–80
- Scharfetter H, Lackner H K and Rosell J 2001a Magnetic induction tomography: hardware for multi-frequency measurements in biological tissues *Physiol. Meas.* **22** 131–46